OXFORD

Cerebral Cortex, May 2021;31: 2720–2728

doi: 10.1093/cercor/bhaa386
Advance Access Publication Date: 31 December 2020
Original Article

ORIGINAL ARTICLE

Dual-Factor Representation of the Environmental Context in the Retrosplenial Cortex

Adam M. P. Miller, Anna C. Serrichio and David M. Smith

Department of Psychology, Cornell University, Ithaca, NY 14853, USA

Address correspondence to David M. Smith, Cornell University, Department of Psychology, 236 Uris Hall, Ithaca, NY 14853, USA. Email: dms248@cornell.edu.

Abstract

The retrosplenial cortex (RSC) is thought to be involved in a variety of spatial and contextual memory processes. However, we do not know how contextual information might be encoded in the RSC or whether the RSC representations may be distinct from context representations seen in other brain regions such as the hippocampus. We recorded RSC neuronal responses while rats explored different environments and discovered 2 kinds of context representations: one involving a novel rate code in which neurons reliably fire at a higher rate in the preferred context regardless of spatial location, and a second involving context-dependent spatial firing patterns similar to those seen in the hippocampus. This suggests that the RSC employs a unique dual-factor representational mechanism to support contextual memory.

Key words: context, memory, population coding, retrosplenial cortex, spatial navigation

Introduction

The retrosplenial cortex (RSC) is critically involved in spatial and contextual memory. RSC damage impairs spatial memory in rodents (Keene and Bucci 2009; Pothuizen et al. 2010) and the RSC is active during spatial navigation tasks in rodents and humans (Epstein et al. 2007; Auger et al. 2015; Milczarek et al. 2018; Miller et al. 2019). The RSC has also been implicated in memory for experimental contexts, which are typically defined by spatial geometry along with nonspatial background features of the environment (e.g., color). RSC lesions impair contextual memory (Keene and Bucci 2008; Kwapis et al. 2015; Robinson et al. 2018; Corcoran et al. 2011) and optogenetic reactivation of RSC neurons is sufficient to evoke a previously learned contextual fear memory (Cowansage et al. 2014). Functional magnetic resonance imaging data from human subjects also suggest that the RSC is involved in contextual memory (Bar and Aminoff 2003; Kim and Maguire 2018).

Despite the evidence for an RSC role in context, we do not know how contextual information might be encoded there. The hippocampus has a well-documented role in contextual memory (Hirsh 1974) which is thought to be supported by context-unique patterns of activity (Smith and Bulkin 2014). For example, when rats explore 2 distinct environments hippocampal neurons exhibit different spatial firing patterns for each environment (i.e., remapping, Leutgeb et al. 2005). Recent work has shown that RSC neurons exhibit spatial firing patterns (Alexander and Nitz 2015; Mao et al. 2018; Miller et al. 2019) which could also serve as a substrate for contextual memory. However, we do not know whether these firing patterns undergo remapping in response to context change or whether some other coding mechanism may support contextual memory. In the present study, we recorded RSC neuronal firing patterns while rats explored 2 different environments. We discovered that the RSC uses a multifaceted population code to represent contexts, including a novel rate code for the context as well as hippocampus-like remapping.

Material and Methods

Subjects and Surgery

Subjects were 4 adult male Long Evans rats (Charles River Laboratories, Wilmington, MA, USA) implanted with custom-built electrode microdrives containing 20 moveable tetrodes made from 17 µm platinum/iridium (90/10%) wire, platinum plated to an impedance of 50–300 kΩ, and arranged in two 10-tetrode linear arrays (one per hemisphere) angled 30° toward the midline and spanning approximately 4 mm along the rostrocaudal axis of the brain (2–6 mm posterior to Bregma, ±1.5 mm lateral).

Tetrodes were lowered into the RSC (35–70 μm daily) until a depth of at least 1 mm was reached. Tetrodes were lowered after every recording session (~15–30 μm) in order to maximize the number of unique neurons recorded. Recording locations are shown in Supplementary Figure S1.

Apparatus, Behavioral Procedures, and Neuronal Recordings

We recorded a total of 146 RSC neurons from 4 rats. Behavioral measures, numbers of neurons, and key results are shown separately for each subject in Supplementary Figures S2 and S3. Consistent with our previous studies (Vedder et al. 2017; Miller et al. 2019), recordings were primarily targeted at the granular b (RSGb) subregion although some records were also taken in the agranular subregion (see Supplementary Fig. S1). We classified putative pyramidal neurons and interneurons according to spike width (Brennan et al. 2020). There were no apparent regional differences or differences across cell types in the context-dependent firing properties we examined, so neurons from both regions and cell types were included in our analyses (see Supplementary Fig. S6C for details). Recordings were obtained while the rats foraged for chocolate sprinkles in 2 distinct PVC boxes measuring (1 m × 1 m × 0.5 m deep) that differed in the color of the box (black or white), the color of the surrounding walls/curtains (white or black), background masking noise (pink or white noise), and ambient odor left by wiping the boxes with baby wipes of different scents (Rite Aid, Inc.). During the approximately 3 min ITI, the rat was placed in an opaque cylinder (30 × 65 cm). Daily recording sessions involved four 12 min trials, 2 in each context, during which neuronal spike data and video data were collected (Digital Cheetah Data Acquisition System, Neuralynx, Inc. Bozeman, MT, USA). The 2 contexts (black and white) were presented in a counterbalanced, randomized sequence for each recording session, although the data are illustrated in ABAB sequence for clarity.

Data Analyses

Context-Dependent Spatial Coding

Spatial firing rate maps for each neuron were constructed by summing the total number of spikes that occurred in a spatial bin (2.5 × 2.5 cm), dividing by the amount of time spent in that bin and then smoothing the data (Skaggs et al. 1996). Pixels that were not visited were excluded from the analysis. Correlations (Pearson's *r*) were computed to compare spatial firing patterns for each pair of trials involving visits to the same context and visits to different contexts. The resulting *r*-values were averaged to create one correlation reflecting within-context similarity and one reflecting between-context similarity for each neuron.

Population coding was assessed using a minimum distance classifier. Population firing rate vectors for every 250 msec time window during the recording session were constructed by combining neurons across subjects and sessions. Firing rates from every neuron were z-scored across all time windows to control for differences in baseline firing rates, which render population variance and distance measures overly sensitive to a few neurons with high firing rates. Time windows from each session were then sorted according to which context (black or white) and spatial bin (36 bins) the rat was in during that time window. Larger spatial bins (17 cm × 17 cm) were used for this analysis so that a sufficient number of visits could be accumulated to train the classifier. Because rats differed in the number of visits they made to each pixel, only 40 visits (250 msec time windows) from each spatial bin in each context were included in the analysis (20 from each trial, drawn at equal intervals across the duration of each trial). When a rat made more than 20 visits to a spatial bin, we preferentially selected visits where the average spatial location of the rat was closer to the center of the bin to avoid including time windows that contained spiking activity from multiple bins. This resulted in 1440 firing rate vectors during each of the 4 context trials (6 pixels × 6 pixels × 20 time windows), representing the instantaneous population firing patterns observed across all the spatial locations. We then computed the mean firing rate vector for each spatial bin in each of the 4 trials (White 1, White 2, Black 1, and Black 2), reflecting the average population firing pattern at each location. We then classified each of the 1440 individual vectors into spatial bins according to which average vector was the most similar (i.e., the smallest Euclidean distance). For within-context classification, we compared the individual vectors to the mean vector for the other trial in the same context (e.g., individual vectors from Black 1 were classified according to the average firing patterns for Black 2). For between-context classification, we found the distances to spatial bins occurring within the opposite context (e.g., individual vectors from Black visits were classified according to the average firing patterns for White visits). This procedure yielded a measure of the degree to which instantaneous population firing patterns matched the typical (average) firing pattern for the same location during the other visit to the same context and for visits to the opposite context. They therefore reflect how stable and reliable the spatial firing patterns are within and between contexts. Classification errors were counted when the instantaneous pattern was most similar to an incorrect spatial bin and spatial error was computed as the distance (in cm) between bin centers of the classified bin and the actual bin.

Rate Coding of the Contexts

The context preference for individual neurons was measured as the normalized difference in firing rates for visits to different contexts and for visits to the same context, computed as the average difference between the firing rates observed in the 2 trials of interest (e.g., Black vs. White or Black 1 vs. Black 2), in 250 msec bins, divided by the standard error. Rate coding was assessed at the population level by combining neurons from all the subjects and sessions and computing population vectors containing the normalized (z-scored) firing rates for each 250 msec time window, resulting in 2880 firing rate vectors for each of the four 12 min trials of the session. We also computed the mean firing rate vector for each of the 4 trials (White 1, White 2, Black 1, and Black 2). We then computed the Euclidean distance between each of the 2880 vectors from one trial (e.g., Black 1) and the mean vector from the other trial of the same context (e.g., Black 2) and the opposite context (White). This yielded a measure of the similarity between each instantaneous firing pattern and the overall (mean) firing pattern for the black and white contexts. Individual firing rate vectors were classified according to the most similar context (smallest distance) and classification errors were counted when the smallest distance was to the opposite context.

Linear–Nonlinear Model

We modeled the effects of multiple behavioral variables on the firing rates of single RSC cells with a linear–nonlinear (L–N) model developed by Hardcastle et al. (2017) for use in the medial entorhinal cortex. This approach is particularly useful for assessing the firing properties of cortical neurons that respond to complex combinations of behavioral and experimental variables. It allows for the independent assessment of how each variable or combination of variables influences neuronal firing. Briefly, the model estimates the firing rate of an individual neuron as a function of the value of each variable of interest (context, head direction, velocity, position, angular velocity, and acceleration). For each neuron, one model was generated for every possible combination of variables (64 models total) and then these models were compared against one another by computing the log-likelihood of held-out data under the model, and penalizing models that over-fit the data. Neurons were then classified in terms of which variables were significantly encoded (Supplementary Fig. S4*H*). A model-derived tuning curve was also obtained for each neuron and variable, which describes how behavior variables translate into firing rates for the neuron. These model-derived firing rates were used to illustrate context-dependent firing rates independent of other variables in Figures 2*C* and 3, but all formal analyses and statistical tests were performed on actual observed firing rates.

Results

Many RSC neurons exhibited clear spatial firing patterns that differed across the 2 contexts (Fig. 1*A*, neurons 1–3) and pixel-by-pixel spatial correlations were significantly higher for visits to the same context (e.g., Black 1 vs. Black 2) than for visits to different contexts (Black vs. White, $t_{(145)} = 8.89$, $P < 0.001$, Fig. 1*C*). Interestingly, response patterns varied widely across neurons in a manner suggestive of a distributed population-level representation. Spatial firing took the form of high baseline firing rates with relatively large regions of elevated firing, consistent with previous reports (Miller et al. 2019), and many neurons showed modest amounts of spatial specificity (Fig. 1, neurons 4–5) or none at all. The neurons also varied in terms of their context-specificity, with some neurons apparently insensitive to context change (Fig. 1, neurons 6–8). Despite this heterogeneity of response patterns, the RSC population as a whole exhibited clear evidence of context-specific spatial firing, with a large majority of neurons (82.12%) showing greater similarity for visits to the same context than for visits to different contexts (Fig. 1*B*, circles above the unity line).

In order to explicitly examine population-level firing patterns, we combined the neurons from all rats into a single population and tested spatial firing patterns using a minimum distance classifier. If the neural population reliably exhibits unique firing patterns at each spatial location, then it should be possible to match a sample of firing data from a subsequent visit to the correct location. In contrast, if the firing at a given location was not reliable and instead varied from one visit to the next, then classification would fall to chance. We applied this logic to assess context-dependent spatial firing patterns by dividing the environment into a 6×6 grid and generating a map of the average population firing pattern at each location for each trial. We then took brief samples (250 msec) of firing data from the other trials and attempted to decode the rat's location by comparing the samples to the original map. By applying the classifier to trials from the same context (e.g., Black 1 and Black 2), we could determine how reliably the spatial firing patterns were expressed within a context. Classification using trials from different contexts (e.g., Black 1 and White 1) revealed how similar or distinct spatial firing patterns were for the 2 different contexts.

We found that classification using trails from the same context correctly decoded the rat's current position far more often than expected by chance (24.62%, compared to chance success rate of 2.80% obtained by shuffling spatial bin labels, binomial test $P < 0.001$; Fig. 1*D*, *E*). The correct spatial bin was the most frequently decoded location, followed by the adjacent spatial bins (Supplementary Fig. S4). Decoding accuracy declined significantly when we attempted to use spatial firing patterns from one context to decode the rat's location in the other context ($t_{(2879)} = 14.07$, $P < 0.001$, *t*-test on distributions of spatial distance errors), indicating that spatial firing patterns were distinct in the 2 contexts. However, decoding accuracy remained above chance even for different contexts (11.58% correct compared to a chance rate of 2.80%, binomial test $P < 0.001$), suggesting that some spatial information is preserved across these 2 contexts. This pattern of results is consistent with the correlation analysis reported above. Both single neuron and population-level analyses indicate consistent spatial firing within each context and distinct firing patterns for different contexts.

Many RSC neurons exhibited reliably higher firing rates in 1 of the 2 contexts (Fig. 2*A*), suggesting a possible rate coding mechanism for differentiating the contexts. We examined this by binning the firing rates for each neuron and trial into twelve 60 s time bins, regardless of spatial position, and we compared the firing rates across trials. Binning the data according to time rather than space revealed consistent contextual difference in firing rates that were not attributable to ongoing behavior or spatial location since these factors are largely independent of time. Analogous to the spatial correlations above, the firing rates of RSC neurons showed greater divergence for visits to different contexts than across visits to the same context (Fig. 2*B*, points above the unity line) and between-context firing rate differences were significantly greater than within-context differences ($t_{(145)} = 4.77$, $P < 0.001$). As with the spatial coding, variability in the rate coding responses across neurons suggested a distributed population representation. The rate differences varied from a strong preference for the black context to a strong preference for the white context, with similar numbers of neurons preferring each (Supplementary Fig. S5*A*).

We examined rate coding at the population level by combining data from all rats and neurons into a single population and computing firing rate vectors for every 250 msec time window. We then computed the Euclidean distance between the population vector for each time window and the mean population vector for the black and white contexts. This allowed us to ask whether the pattern of firing rates across the neural population at each moment in time was more similar to the average white box firing pattern or black box pattern. We found that the population firing patterns were nearly always more similar to the mean of the same context than of the opposite context, which allowed us to correctly classify any population vector as having come from the black box or the white box over 90% of the time (Fig. 2*D*, $P < 0.001$, compared to a control distribution obtained by shuffling context labels). Therefore, despite considerable moment to moment variability in firing patterns resulting from differences in behavior and spatial location, there was an overriding consistency within each context that could easily

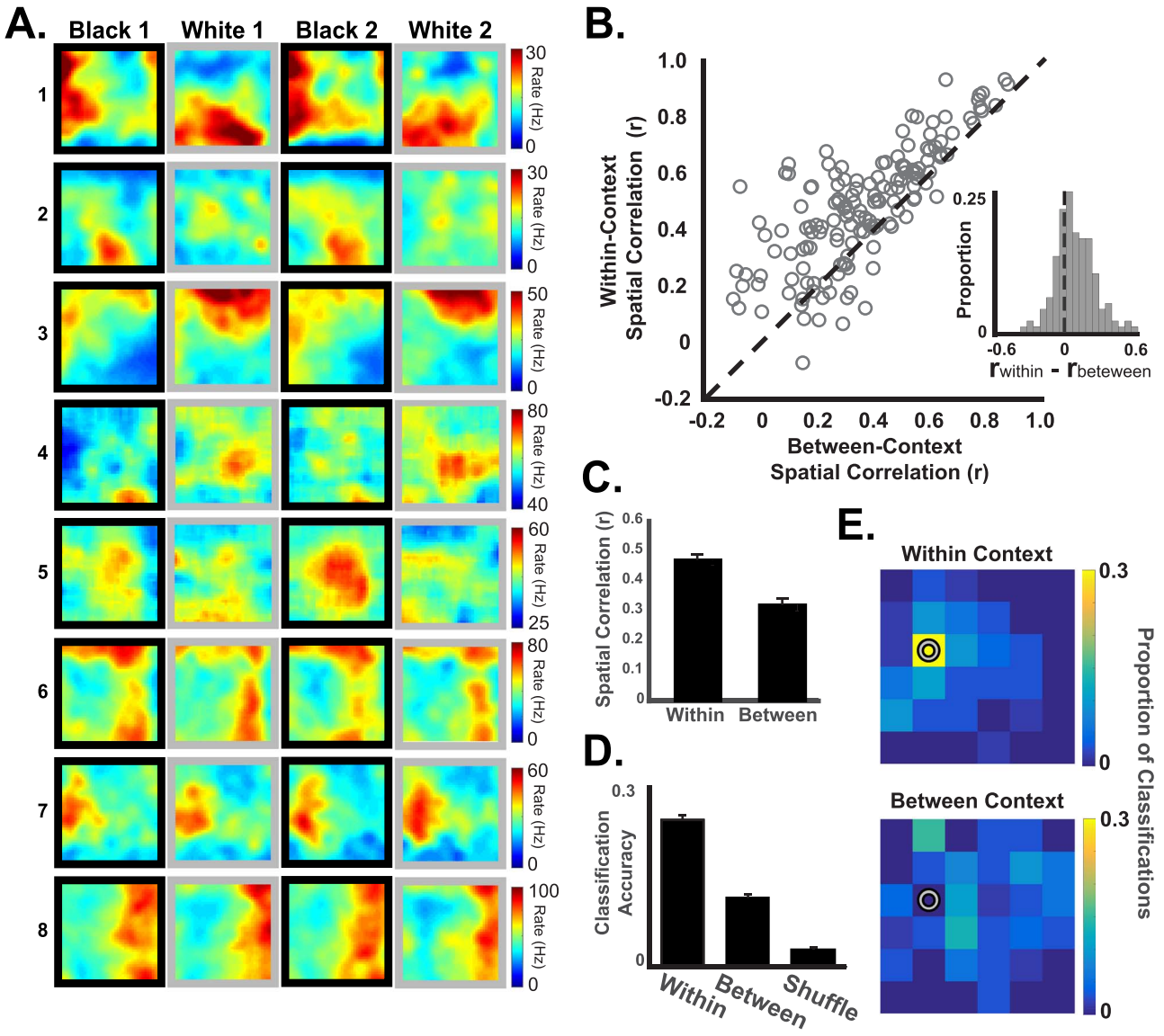

Figure 1. Retrosplenial cortical neurons exhibit context-specific spatial coding. (*A*) Spatial firing rate maps from illustrative examples of spatial firing patterns in the black and white contexts. Some neurons (e.g., neurons 1–3) exhibited spatially localized firing that was context dependent, whereas others (4–5) exhibited less spatial specificity (note that the color scale starts above 0). Some neurons (e.g., 6–8) exhibited spatial firing patterns that were not context dependent. Plots are shown in Black-White-Black-White order for illustration. The actual order of black and white trials was randomized. (*B*) Pixel-by-pixel correlations (open circles) of firing rate maps for trials occurring in the same context (*y*-axis) and different contexts (*x*-axis). Most neurons exhibited more similar spatial firing for visits to the same context than for different contexts (circles above the unity line and inset). (*C*) Average within-context correlations were significantly higher than between-context correlations. (*D*) Decoding of the rat's current position from population activity patterns was more accurate when the classifier was trained on data from the same context (within) than when trained on data from the different context (between) and compared to shuffled data. (*E*) Heat maps illustrating an example of successful decoding of the current position (pixel with a circle) using same-context data (top) as compared to different-context data. One example location is shown here. See Supplementary Figure S4 for all other locations.

be decoded. Principal components analysis produced the same pattern of results, with distinct firing patterns for the black and white contexts (Supplementary Fig. S5C).

RSC neurons exhibited 2 types of context-specificity, context-dependent spatial firing patterns and context-dependent rate coding. Measures of these types of context coding were not correlated ($r = 0.01$, $P = 0.89$, also see Supplementary Fig. S6A, B) and individual neurons could have a strong rate code, a strong spatial code, neither or both (Fig. 3). Many neurons exhibited only small or moderate amounts spatial or rate coding of the context, and a substantial minority of neurons did not carry contextual information of either type (circles near or below zero). However, a majority of neurons differentiated the contexts on one or both dimensions (Fig. 3, upper right quadrant), suggesting that contextual information is carried by a distributed population code which does not depend solely on a small number of neurons with strong spatial or rate coding.

Previous studies indicate that individual RSC neurons exhibit complex response patterns that are influenced by a variety of task variables (Alexander and Nitz 2017; Vedder et al. 2017;

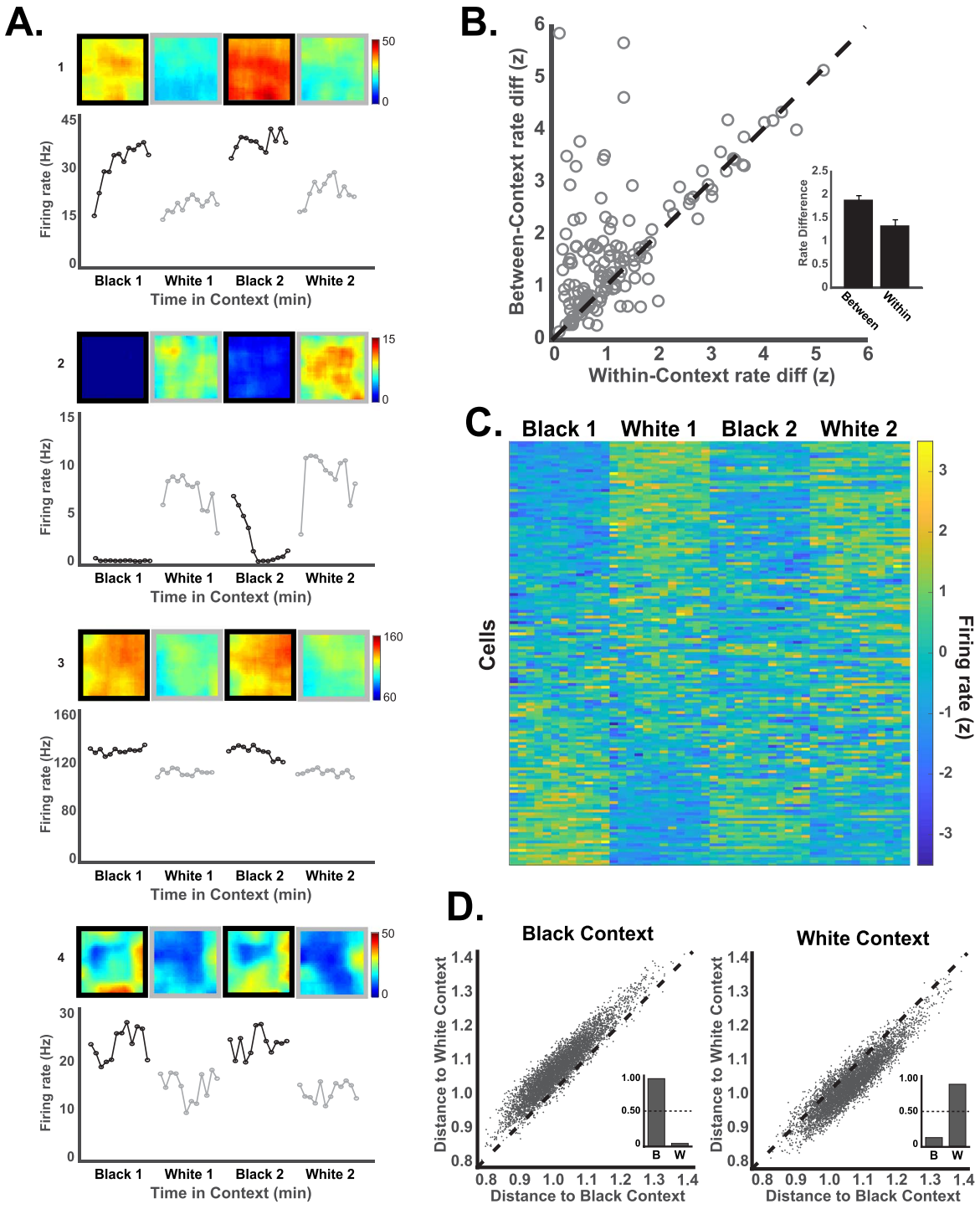

Figure 2. RSC neurons exhibit a rate code for the context. (*A*) Example neurons illustrating rate coding of the context. For each neuron, the spatial firing rate map is shown above and the average firing rate for the 12 consecutive minutes of each trial is shown in the line plots below. Many rate coding neurons (e.g., 1–3) exhibited little spatial selectivity within the environment, but some neurons exhibited spatial firing with different overall rates in the 2 contexts (e.g., neuron 4 which fired near the walls). (*B*) Firing rate differences for visits to the black and white contexts (between-context rate differences) are plotted against firing rate differences for visits to the same context (within-context rate differences) for each neuron (circles). Greater differentiation of the 2 contexts, as compared to within-context baseline variability, is indicated by circles above the unity line. Average within- and between-context firing rate differences are shown in the inset. (*C*) Firing rates across the 4 trials are shown for all neurons in 1 min time windows sorted by firing rate in the first black context trial. The influence of noncontextual variables (e.g., running speed) was statistically removed for illustration (see L–N model methods and Fig. 4). (*D*) Population firing patterns (250 msec vectors) are plotted in terms of their distance from the mean representation of the black and white contexts. Individual population vectors from the black context (left) were nearly always closer to the average black context representation (dots above the unity line). The inset shows the proportion of population vectors accurately classified as having come from the black context (*B*) and erroneous classifications to the white context (W). The reverse is seen for population vectors taken from the white context (right).

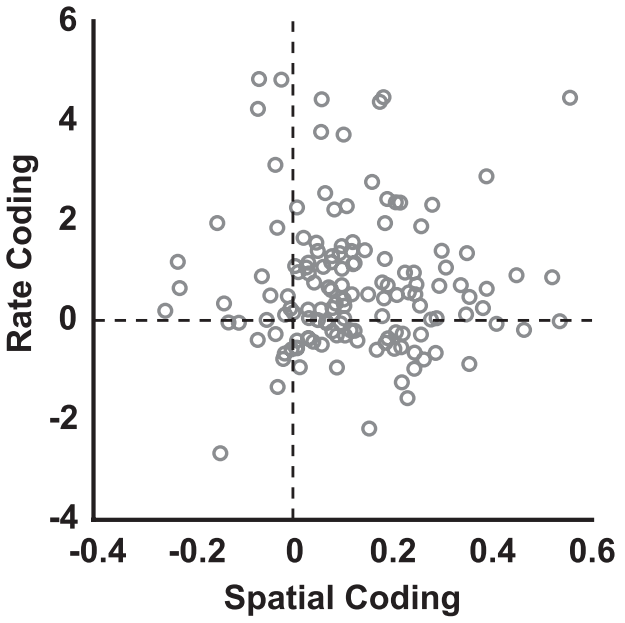

Figure 3. Individual neurons (circles) exhibited varying degrees of spatial coding and rate coding of the contexts. Spatial coding of the context (*x*-axis) is computed as the between-context spatial correlation minus the within-context correlation (r_{within}—$r_{between}$). Positive numbers indicate greater within-context similarity of firing patterns, as compared to between contexts. Rate coding (*y*-axis) is computed as the between-context rate difference minus the within-context rate difference. Positive numbers indicate greater firing rate differentiation of the contexts, as compared to baseline firing rate variability across visits to the same context. All firing rates were normalized (*z*-scored) and the influence of noncontextual variables (e.g., running speed) was statistically removed for illustration using the L–N model, as in Figure 2C.

Miller et al. 2019). This can include behavioral variables such as running speed, acceleration, angular velocity, and heading direction. It was therefore important to rule out the possibility that the apparent contextual differences instead reflect systematic behavioral differences between the 2 contexts. We examined the behavior of each subject and found that behavior was broadly similar across contexts although some subjects did exhibit behavioral differences (Supplementary Fig. S2). In order to formally assess the influence of these behavioral variables, we applied a statistical approach designed to independently assess the influence of multiple behavioral variables on neuronal firing (Hardcastle et al. 2017, see L–N model in Methods). The firing rate of each neuron was decomposed into separate tuning curves for each variable. Then individual variables were sequentially added to our model only if they significantly improved the ability of the model to predict firing. Thus, any number of variables can be found to influence firing but those that have no significant influence are excluded. We found that more than half of the neurons carried a significant amount of information about spatial location, context, velocity, and head direction, whereas a smaller proportion carried information about angular velocity and acceleration (Fig. 4A), and most neurons (84%) carried information about 2 or more of these variables simultaneously. Importantly, 58% of the neurons significantly encoded the context, even after accounting for the influence of running speed and other behavioral variables. This suggests RSC neuronal firing carries a clear contextual signal that is readily apparent despite the influence of noncontextual behavioral variables. For example, neuronal firing is strongly correlated with running

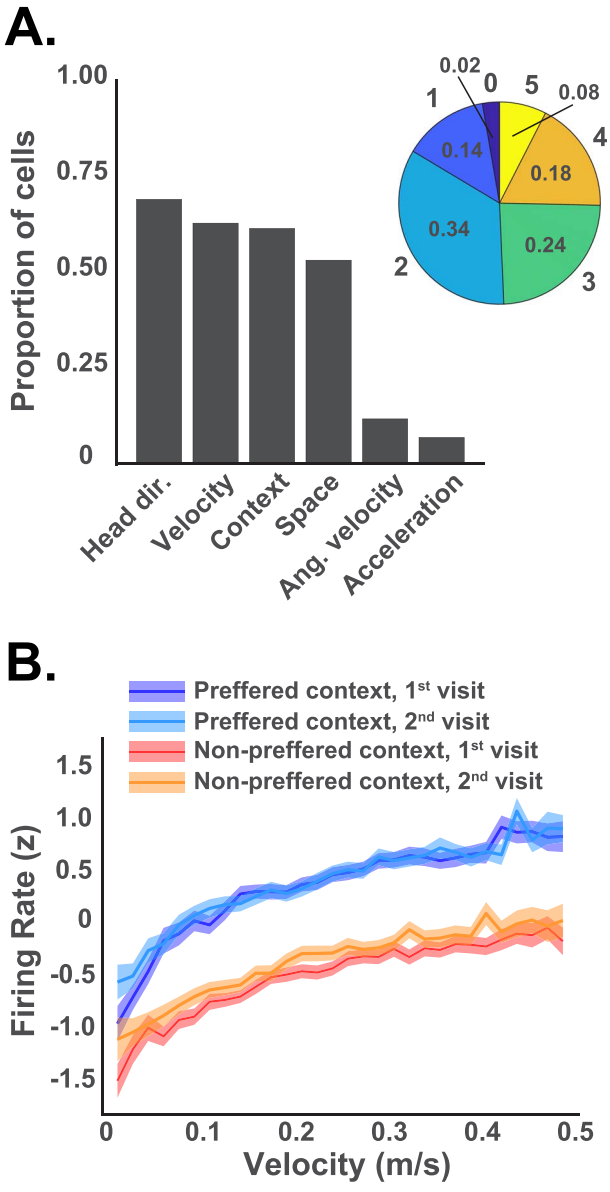

Figure 4. (*A*) The bar plot indicates the number of neurons that significantly encoded each of the 6 behavioral and task variables, as indicated by the L–N analysis. Most neurons encoded more than one of these variables, with the majority encoding 2 or 3. The pie chart shows the proportion of neurons that encoded different numbers of the 6 variables. Only 2% of the neurons encoded none of the variables and none encoded all 6. (*B*) Average firing rates for all context coding neurons (identified by the L–N model) are plotted across the range of running speeds. Separate lines are shown for the 2 visits to the preferred context (i.e., the context with the highest firing rate) and the 2 visits to the nonpreferred context with SEM indicated by shading. Note that the firing rates clearly differentiated the 2 contexts at any given running speed.

speed, even in the neurons that significantly encoded context, but the effect of context is nevertheless apparent across all speeds (Fig. 4B, also see Supplementary Fig S2B).

Discussion

RSC neurons exhibited a clear population-level representation of the environmental context, the loss of which could readily

explain contextual memory deficits in subjects with lesions (Keene and Bucci 2008; Nelson et al. 2014; Kwapis et al. 2015; Robinson et al. 2018). This involved 2 distinct types of context-specificity, spatial coding, and rate coding. The robust rate code for the context was a surprising finding. We know of no other instances where rate coding is used to differentiate complex multidimensional variables like the environmental context, and the RSC rate code was so reliable that we could accurately distinguish the contexts from just a brief glimpse of the firing pattern. Although hippocampal neurons exhibit rate coding, it involves firing rate changes within the neuron's place field and seems to reflect a kind of partial remapping of spatial firing patterns in response to relatively small changes in the environment (Leutgeb et al. 2005). In contrast, the RSC rate code provides an unambiguous context-discriminating signal that is independent of spatial location within the environment. This clear and simple context signal could readily be used by other brain regions to modulate processing according to the current context.

Interestingly, rate coding neurons may explain why optogenetic reactivation of the RSC can effectively evoke contextual memories (Cowansage et al. 2014). The endogenous firing patterns of many neural populations involve precise temporal or spatial patterning, which is quite different from artificial reactivation patterns. In contrast, some RSC rate coding neurons show little spatial or temporal patterning, so artificial reactivation of these neurons could provide a contextual signal that is similar to the endogenous signal. Hippocampal reactivation may also reactivate RSC rate coding neurons through extensive direct and indirect connections between the 2 structures (Wyss and Groen 1992). Consistent with this idea, reactivation of RSC neurons is sufficient to evoke contextual memories even without the hippocampus (Cowansage et al. 2014).

Previous studies have shown that RSC neurons generate a population-level representation of the current location within the environment (Alexander and Nitz 2015; Mao et al. 2018; Miller et al. 2019). However, these studies employed mazes in which sensory and motor variables such as running speed, head direction, and optic flow are invariably confounded with location, so it is notable that we found similar spatial representations in the RSC during unconstrained exploration in an open field where these variables are less likely to account for spatial firing patterns. As with previous studies, RSC neurons did not exhibit discrete, highly specific place fields like those seen in the hippocampus. Instead, they fired across broad regions of the environment with reliably higher rates in some regions and lower rates in others. Consistent with recent reports of RSC boundary coding (Alexander et al. 2020), many neurons had regions of elevated firing near the walls and these firing patterns also appeared to be sensitive to the context manipulation (see Figs. 1A and 2A).

The RSC spatial representations differentiated the 2 contexts in a manner similar to the hippocampus (Leutgeb et al. 2005), with many RSC neurons exhibiting clear remapping across the 2 contexts (Fig. 1A). However, the amount of remapping varied and some neurons had spatial firing patterns that were insensitive to the context manipulation. This resulted in firing patterns that were considerably more similar for the black and white contexts than would be expected in the hippocampus. Average within-context correlation coefficients were similar to those seen in previous studies of the hippocampus using the same context manipulations but between-context correlations were substantially higher (RSC mean = 0.32, compared to 0.05 in the hippocampus, Law et al. 2016). Consequently, we were able to use the firing patterns in one context to predict the rat's location in the other context at above-chance levels, suggesting that some spatial information is preserved across different contexts. This suggests that RSC spatial representations may not reflect the kind of pattern separation seen in the hippocampus. Instead, RSC neurons may encode both the stable features, such as the shape of the box, as well as the differences between the contexts.

RSC lesions have been shown to disrupt contextual memory across a range of experimental methods and varying environmental cue manipulations (Keene and Bucci 2008; Nelson et al. 2014; Kwapis et al. 2015; Robinson et al. 2018). Like previous studies, our context manipulation involved changes in several environmental cues of different modalities (box color, background color of distal walls, odor, and background masking noise) so we do not know how much each of the individual cues might have contributed to RSC representations. The RSC receives extensive input from the visual system and RSC neurons respond to visual stimuli (Zhuang et al. 2017; Powell et al. 2020), suggesting that visual input may play a dominant role in the RSC representations. However, visual information is not the sole determinant: RSC spatial representations persist after removal of visual information (i.e., in darkness, Mao et al. 2018) and conversely, RSC representations readily differentiate distinct goals even when visual input is the same (Miller et al. 2019). The RSC also receives auditory input and there is an extensive literature on RSC responses to auditory cues (e.g., Duvel et al. 2001; Todd et al. 2016). Less is known about the RSC role in processing olfactory cues. However, studies of mating and pair bonding, where olfaction is known to be critical, have implicated the RSC (Parker et al. 2011; Ophir 2017). More recently, studies have shown that the RSC is necessary for forming associations between auditory and visual stimuli that occur together (Robinson et al. 2014; also see Hindley et al. 2014; Nelson et al. 2015) and the capacity to bind diverse stimuli together could be the foundation for generating coherent context representations (Todd et al. 2017). Further study is needed to quantify the degree to which RSC neurons encode various cues and cue conjunctions, but our finding that RSC representations are responsive to changes in an array of contextual variables is consistent with this idea.

Supplementary Material

Supplementary material can be found at *Cerebral Cortex* online.

Notes

A.M.P.M., A.C.S., and D.M.S. designed the experiments. A.M.P.M. and D.M.S. wrote the paper. A.M.P.M. and A.C.S. conducted the experiments. A.M.P.M. performed the analyses. We thank Alexandra Tse for assistance with animal training and electrode microdrive fabrication.

Conflict of interest: The authors declare no conflict of interest.

Funding

National Institutes of Health (grant R01 MH083809 to D.M.S).

References

Alexander AS, Carstensen LC, Hinman JR, Raudies F, Chapman GW, Hasselmo ME. 2020. Egocentric boundary vector tuning

of the retrosplenial cortex. *Sci Adv*. 6(8): eaaz2322. Available from: http://www.ncbi.nlm. nih.gov/pubmed/32128423

Alexander AS, Nitz DA. 2015. Retrosplenial cortex maps the conjunction of internal and external spaces. *Nat Neurosci*. 18:1143–1151. Available from. http://www.ncbi.nlm.nih.gov/pubmed/26147532.

Alexander AS, Nitz DA. 2017. Spatially periodic activation patterns of retrosplenial cortex encode route sub-spaces and distance Traveled. *Curr Biol*. 27:1551–1560.e4. Available from: http://www.ncbi.nlm.nih.gov/pubmed/28528904

Auger SD, Zeidman P, Maguire EA. 2015. A central role for the retrosplenial cortex in de novo environmental learning. *Elife*. 4. Available from:. http://www.ncbi.nlm.nih.gov/pubmed/26284602.

Bar M, Aminoff E. 2003. Cortical analysis of visual context. *Neuron*. 38:347–358.

Brennan EKW, Sudhakar SK, Jedrasiak-Cape I, John TT, Ahmed OJ. 2020. Hyperexcitable neurons enable precise and persistent information encoding in the superficial retrosplenial cortex. *Cell Rep*. 30:1598–1612.e8.

Corcoran KA, Donnan MD, Tronson NC, Guzma YF, Gao C, Jovasevic V, Guedea AL, Radulovic J. 2011. NMDA Receptors in Retrosplenial Cortex Are Necessary for Retrieval of Recent and Remote Context Fear Memory. *J Neurosci*. 31(32):11655–11659. Available from: https://pubmed.ncbi.nlm.nih.gov/21832195.

Cowansage KK, Shuman T, Dillingham BC, Chang A, Golshani P, Mayford M. 2014. Direct reactivation of a coherent neocortical memory of context. *Neuron*. 84:432–441. Available from. http://www.ncbi.nlm.nih.gov/pubmed/25308330.

Duvel A, Smith DM, Talk A, Gabriel M. 2001. Medial geniculate, amygdalar and cingulate cortical training-induced neuronal activity during discriminative avoidance learning in rabbits with auditory cortical lesions. *J Neurosci*. 21:3271–3281.

Epstein RA, Parker WE, Feiler AM. 2007. Where am i now? Distinct roles for parahippocampal and retrosplenial cortices in place recognition. *J Neurosci*. 27:6141–6149. Available from. http://www.ncbi.nlm.nih.gov/pubmed/17553986.

Hardcastle K, Maheswaranathan N, Ganguli S, Giocomo LM. 2017. A multiplexed, heterogeneous, and adaptive code for navigation in medial Entorhinal cortex. *Neuron*. 94:375–387.e7. Available from. http://www.ncbi.nlm.nih.gov/pubmed/28392071.

Hindley EL, Nelson AJD, Aggleton JP, Vann SD. 2014. Dysgranular retrosplenial cortex lesions in rats disrupt cross-modal object recognition. *Learn Mem*. 21:171–179. Available from. http://www.ncbi.nlm.nih.gov/pubmed/24554671.

Hirsh R. 1974. The hippocampus and contextual retrieval of information from memory: a theory. *Behav Biol*. 12:421–444.

Keene CS, Bucci DJ. 2008. Contributions of the retrosplenial and posterior parietal cortices to cue-specific and contextual fear conditioning. *Behav Neurosci*. 122:89–97. Available from. http://www.ncbi.nlm.nih.gov/pubmed/18298252.

Keene CS, Bucci DJ. 2009. Damage to the retrosplenial cortex produces specific impairments in spatial working memory. *Neurobiol Learn Mem*. 91:408–414.

Kim M, Maguire EA. 2018. Hippocampus, retrosplenial and parahippocampal cortices encode multicompartment 3D space in a hierarchical manner. *Cereb Cortex*. 28:1898–1909. Available from. http://www.ncbi.nlm.nih.gov/pubmed/29554231.

Kwapis JL, Jarome TJ, Lee JL, Helmstetter FJ. 2015. The retrosplenial cortex is involved in the formation of memory for context and trace fear conditioning. *Neurobiol Learn Mem*. 123:110–116. Available from. https://pubmed.ncbi.nlm.nih.gov/26079095/.

Law LM, Bulkin DA, Smith DM. 2016. Slow stabilization of concurrently acquired hippocampal context representations. *Hippocampus*. 26:1560–1569. Available from. http://www.ncbi.nlm.nih.gov/pubmed/27650572.

Leutgeb S, Leutgeb JK, Barnes CA, Moser EI, McNaughton BL, Moser MB. 2005. Independent codes for spatial and episodic memory in hippocampal neuronal ensembles. *Science*. 309:619–623.

Mao D, Neumann AR, Sun J, Bonin V, Mohajerani MH, McNaughton BL. 2018. Hippocampus-dependent emergence of spatial sequence coding in retrosplenial cortex. *Proc Natl Acad Sci USA*. 115:8015–8018.

Milczarek MM, Vann SD, Sengpiel F. 2018. Spatial memory engram in the mouse Retrosplenial cortex. *Curr Biol*. 28:1975–1980.e6. Available from. http://www.ncbi.nlm.nih.gov/pubmed/29887312.

Miller AMP, Mau W, Smith DM. 2019. Retrosplenial cortical representations of space and future goal locations develop with learning. *Curr Biol*. 29:2083–2090.e4. Available from. http://www.ncbi.nlm.nih.gov/pubmed/31178316.

Nelson AJD, Hindley EL, Haddon JE, Vann SD, Aggleton JP. 2014. A novel role for the rat retrosplenial cortex in cognitive control. *Learn Mem*. 21:90–97.

Nelson AJD, Powell AL, Holmes JD, Vann SD, Aggleton JP. 2015. What does spatial alternation tell us about retrosplenial cortex function? *Front Behav Neurosci*. 9.

Ophir AG. 2017. Navigating monogamy: nonapeptide sensitivity in a memory neural circuit may shape social behavior and mating decisions. *Front Neurosci*. 11:397. Available from:. https://pubmed.ncbi.nlm.nih.gov/28744194/.

Parker JT, Rodriguez N, Lawal B, Delevan CJ, Bamshad M. 2011. Mating increases male's interest in other females: a cognitive study in socially monogamous prairie voles (Microtus ochrogaster). *Behav Processes*. 88:127–134. Available from. https://pubmed.ncbi.nlm.nih.gov/21888956/.

Pothuizen HHJ, Davies M, Aggleton JP, Vann SD. 2010. Effects of selective granular retrosplenial cortex lesions on spatial working memory in rats. *Behav Brain Res*. 208:566–575. Available from. http://www.ncbi.nlm.nih.gov/pubmed/20074589.

Powell A, Connelly WM, Vasalauskaite A, Nelson AJDD, Vann SD, Aggleton JP, Sengpiel F, Ranson A. 2020. Stable encoding of visual cues in the mouse Retrosplenial cortex. *Cereb Cortex*. 30:4424–4437. Available from. https://pubmed.ncbi.nlm.nih.gov/32147692/.

Robinson S, Adelman JS, Mogul AS, Ihle PCJ, Davino GM. 2018. Putting fear in context: elucidating the role of the retrosplenial cortex in context discrimination in rats. *Neurobiol Learn Mem*. 148:50–59. Available from. https://pubmed.ncbi.nlm.nih.gov/29294384/.

Robinson S, Todd TP, Pasternak AR, Luikart BW, Skelton PD, Urban DJ, Bucci DJ. 2014. Chemogenetic silencing of neurons in retrosplenial cortex disrupts sensory preconditioning. *J Neurosci*. 34:10982–10988. Available from. http://www.ncbi.nlm.nih.gov/pubmed/25122898.

Skaggs WE, McNaughton BL, Wilson MA, Barnes CA. 1996. Theta phase precession in hippocampal neuronal populations and the compression of temporal sequences. *Hippocampus*. 6:149–172.

Smith DM, Bulkin DA. 2014. The form and function of hippocampal context representations. *Neurosci Biobehav Rev*. 40C:52–61.

Todd TP, DeAngeli NE, Jiang MY, Bucci DJ. 2017. Retrograde amnesia of contextual fear conditioning: evidence for retrosplenial cortex involvement in configural processing. *Behav Neurosci*. 131:46–54. Available from. http://www.ncbi.nlm.nih.gov/pubmed/28054807.

Todd TP, Mehlman ML, Keene CS, DeAngeli NE, Bucci DJ. 2016. Retrosplenial cortex is required for the retrieval of remote memory for auditory cues. *Learn Mem*. 23: 278–288. Available from. http://www.ncbi.nlm.nih.gov/pubmed/27194795.

Vedder LC, Miller AMP, Harrison MB, Smith DM. 2017. Retrosplenial cortical neurons encode navigational cues, trajectories and reward locations during goal directed navigation. *Cereb Cortex*. 27:3713–3723. Available from:. http://www.ncbi.nlm.nih.gov/pubmed/27473323.

Wyss JM, Van Groen T. 1992. Connections between the retrosplenial cortex and the hippocampal formation in the rat: a review. *Hippocampus*. 2:1–11. Available from: http://www.ncbi.nlm.nih.gov/entrez/query.fcgi?cmd=Retrieve&db=PubMed&dopt=Citation&list_uids=1308170

Zhuang J, Ng L, Williams D, Valley M, Li Y, Garrett M, Waters J. 2017. An extended retinotopic map of mouse cortex. *Elife*. 6: 1–29. Available from:. https://pubmed.ncbi.nlm.nih.gov/28059700/.